

# Failure Analysis of a Crank Hinge in a Guillotine Machine

A. R. LOKUGE<sup>1</sup>, R. J. WIMALASIRI<sup>2</sup>

(1. *Mechanical Engineering, Department of Mechanical Engineering Kingston University, London;*

2. *Mechanical Engineering, Department of Mechanical Engineering, The Open University of Sri Lanka, Nawala, Nugegoda)*

**Abstract:** Guillotine machines are used to cut bulk quantities of paper, often thousands at a time. More the number of papers to be cut at once, more load is required to cut. This machine undergoes a frequent failure of one of its hinges, which prevents the operation of the machine. A combination of torsional forces and bending moments are acting on the hinge when operating. Torsional stresses induced due to the friction between the contacting surfaces of the crank rod and the hinge. The bending moment induced due to the alternating motion and the load acted upon the cutting mechanism. The crank transforms the rotational movement into a translational motion of the blade, which results in the formation of a cyclic load in the form of a sinusoidal with a mean value not equal to zero. This leads to fail the hinge in the mode of fatigue. Naked eye observations of the fracture surface revealed a clear failure initiation point and striation marks of crack propagation and a sudden fracture region which evident a fatigue failure due to cyclic loading. To redesign the failed hinged to avoid such failure, it is essential to, (i) define and evaluate the stresses developed by the combined loading condition (ii) understand the nature of the cyclic stress induced. The force acting on the hinge was calculated by the law of conservation of momentum created by the blades' inertia and its' supportive structure. It was understood that the mean stress value of the cyclic load is not equal to zero, the modified Goodman diagram is used. Computational simulations are conducted using Finite Element Analysis (FEA) on the ANSYS fatigue tool. By applying the fatigue analysis theories and conducting FEA for stress analysis, the reason for the failure is revealed and then necessary precautions could be taken to prevent such failures in the future.

**Keywords:** Fatigue Fracture, Crack Propagation, Cyclic Load, FEA, Mean Stress.

## 1 Introduction

Guillotine machines are used to cut bulk quantities of paper often thousands at a time. More the number of papers to be cut, more load is required to cut the papers, thereby causing an increase in the required cutting force. Important components in the Guillotine machine (Fig.1) are Flywheel, Induction motor, Clutch,

Crank, Cutting mechanism, Pulley, Gears and Hinges. The flywheel is driven by an induction motor via a pulley drive where the motor is in a continuous rotational mode. The flywheel's main link of transforming the energy of the motor, by preventing the submission of any inertia loads. The repeated engaging and disengaging motion of the crank is ensured by the presence of a clutch while a lever ensures that this con-

tinuous mechanism is under control. A pre-adjusted threaded bar at the end of the rod ensures a controlled movement of the blades. The slider and the crankshaft is connected by a connecting rod. The bolt is used as a hinge, to pivot the rod with the crank. The failure of this hinge occurs frequently mainly due to a combination of torsional and bending loads. Torsional stresses are due to the friction acting between the contacting surfaces of the rod and the hinge and the bending moment induced due to the alternating motion of the cutting blade. The crank transforms the rotational motion into translational motion of the blade, which results in the formation of a pulsating load. This load is in sinusoidal pattern with a mean stress value not equal to zero. These can cause failure in the mode of fatigue. By observing the failed components, it was identified glimpses of crack initiations and beach marks of crack propagation and a sudden ductile fracture which ensures a fatigue failure due to cyclic loading. This modified Goodman diagram is used for the calculations and computational simulations is performed on FEA, on ANSYS fatigue analysis tool.

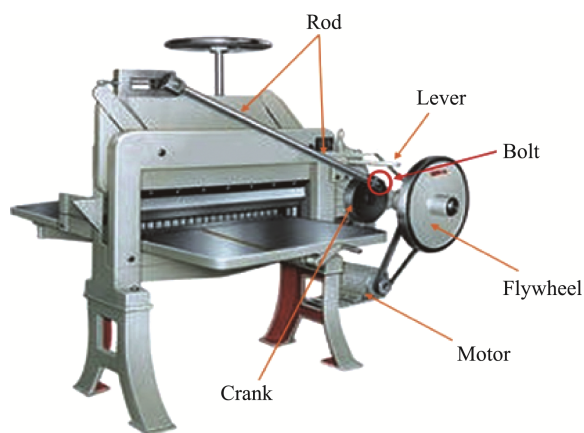


**Fig.1 Illustration of Machine** (Source: <https://toyoprintingmachine.en.made-in-china.com/product/mvknrNBHYgc/China-Dq-201-Mechanical-Paper-Cutting-Machine.html>)

## 2 Literature Review

The process of cycle-by-cycle accumulation of damage in a material that is undergoes fluctuating

stresses and strains, is defined as fatigue failure. Any load is not significantly large enough to cause an immediate failure, is one of the significant features of fatigue <sup>[1-3]</sup>. Failure starts to occur only after a certain number of load fluctuations are experienced, which means that only when the accumulated damage has reached a critical level, then failure initiates <sup>[4]</sup>. Cracks initiation occurs from the surface of a component due to the fatigue damage, which begins from here in the form of shear cracks on crystallographic slip planes. This is known as crack initiation. After the completion of the transition period of crack initiation, crack propagation takes place in a direction normal to the applied stress <sup>[5]</sup>. In the final stage, the crack becomes unstable, and fracture occurs. Fatigue crack propagation is the name given to the process that occurs before fracture. Some of the early stages may be skipped and this is entirely dependent on the initial crack length in a component. The “defect free” metal components are the only components which consist of these five stages of the fatigue process. Fatigue damage is fundamentally caused as a result of structural changes at the microscopic level, such as dislocations of the atomic structures. It is justifiable to assume that the microscopic parameters that govern fatigue damage, possess an inherent relationship with macroscopic stress and strain quantities based on the continuum mechanics concepts. Crack nucleation and early growth, both of which can be accounted for, using these macroscopic quantities. The most important component of fatigue analysis is the relationship between stress amplitude and number of cycles which it can execute, before experiencing failure. S-N curves, are used for this kind of analysis where S denotes stress that is indicated by the Y-axis and the logarithmic of the number of cycles is indicated by the X-axis. The curve is sketched using practically obtained values. The shape of the S-N curve represents that of an exponential decay graph, for a lower number of cycles. There is a sudden deviation after a certain point of the number of cycles and then the S-N curve become parallel to the number of cycles. The point at which the S-N curve deviates is defined as the endurance limit of the material. If engineers keep

the maximum stress levels below the endurance limit, then the component achieves infinite fatigue life [6-7].

There are four major stages which are considered as the process of total fatigue life [8-10]. These four stages are:

1. Nucleation or permanent damage caused by substructural and microstructural. This is also known as initiation or nucleation of fatigue cracks.

2. The creation and growth of microscopic cracks, also known as small-crack growth.

3. The formation of “dominant cracks” due to the growth and coalescence of microscopic flaws and the stable propagation of dominant macrocracks. This is known as Macro-crack propagation.

4. The structural instability or complete failure which can be termed as the final fracture.

The period during which cracks initiate from defects and propagate, is defined as the fatigue life of engineering components and structures. The problem of fatigue failure arising becomes a possibility whenever engineering structures operate under severe conditions. It is during the crack propagation stage that the largest fraction of fatigue life is spent. When operating under severe or extreme conditions, the problem of fatigue failure is raised in engineering structures. The prediction of damage caused by corrosion fatigue during the early stages of damage is an outstanding issue that is yet to be solved in the field of corrosion science and engineering.

However, S-N curves are used only for fully reversible cyclic loads which means the mean value of the load fluctuation is equal to zero [11, 12]. If the stresses induced in a pedal of a bicycle were considered, the mean value of that fluctuating load is not equal to zero. In such a case, it may require Goodman diagrams and ultimately, modified Goodman diagrams [13].

The endurance limit of a material can be determined by the RR Moor testing method. This RR Moor testing method is conducted by the rotation of a specimen made from a particular material about its symmetrical axis, via a motor, with a variable imbalanced mass attached to the specimen. Using the number of cycles and stress denoted by the imbalanced

mass, the S-N curve is obtained [14-15]. Using this obtained S-N curve, the ideal endurance limit value of the material is obtained. The reason this is called the ideal value is due to the three assumptions made during this test. These three assumptions are:

1. Specimen is homogeneous
2. Absence of any defects
3. The surface of the material is highly

In the real scenario, these three assumptions, may not have any validity attached to them due to which materials can undergo failure before the ideal endurance limit value ( $S'_e$ ) obtained via RR Moor testing method. This is why, the endurance value is not considered as much as the value of tensile or shear strength, due to its dependency on a lot of other factors.

To determine a more realistic value for the endurance limit [16], the value of the ideal endurance need to be gained by several coefficients that are less than one [17].

The four major factors are:

1. Surface finish factor ( $K_a$ ) – Effect of scratches on the surface.
2. Size factor ( $K_b$ ) – Effect of surface defects.
3. Stress concentration ( $K_d$ ) – Effect of discontinuity.
4. Reliability factor ( $K_c$ )

The two minor factors are:

1. Factor due to the loading condition
2. Factor due to the temperature condition

The realistic value can be obtained using equation (1).

$$S_e = K_a K_b K_c k_d S'_e \quad (1)$$

When a component or structure is considered a continuum (assumed as free of any cracks), the S-N approach is very appropriate to perform fatigue analysis. The general representation of fatigue process leading to failure, is represented in terms of the crack initiation stage followed by the crack propagation to a critical size [18]. There is no generally accepted definition as to what constitutes the initiation or when the propagation commences when the initiation phase is completed. The combined sum of both, the crack initiation and the propagation are represented by the net

cycles to failure.

$$\text{Total fatigue} = N_i + N_p$$

Where,

$N_i$  – Number of cycles for crack initiation

$N_p$  – Number of cycles for crack propagation to failure

The hinge point experiences a bending moment due to force acting on it created by the movement of the blade. A torsion also induced between the surfaces of the hinge and the connecting rod due to its Friction force. The blade is coming down at an angle of 80 degree and it's called as the shearing angle for the paper to be cut. Total work is done by the flywheel and the total stresses are acting on the hinge. Illustration of the force diagram is shown in Fig.2.

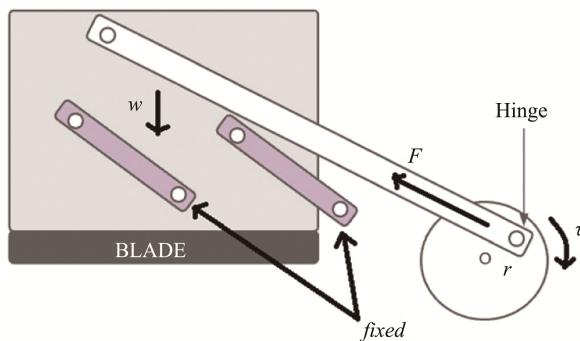


Fig.2 Illustration of the Force Diagram

### 3 Conceptual Approach to Final Solution to the Problem

Fatigue damage is a gradual process which increases in direct proportionality to the applied cycles of loading in a cumulative manner, that may lead to fracture. Cumulative fatigue damage (CFD) is the fundamental theory which is the framework that is used for fatigue strength assessment (FSA). Recent research activities and development work, mooted the, fatigue crack propagation (FCP) theory whose fundamentals were totally based on the fracture mechanics concepts. The fundamental cause of fatigue damage is the material structural changes, which take place at the microscopic level, such as dislocations of the atomic structures. The long term problem is that of the collating

microscopic quantities as well as the macroscopic experimental observations, though it is still possible to percept that the microscopic parameters which govern fatigue damage, possess an inherent relationship with the macroscopic stress and strain quantities<sup>[19, 20]</sup>, that are fundamentally based upon the continuum mechanics concepts. Its these macroscopic quantities that can be used to identify crack nucleation and early crack growth.

On observation of the fracture surface, it is assessed that the failure is due to fatigue. Two different cross sections are shown in Fig.3.

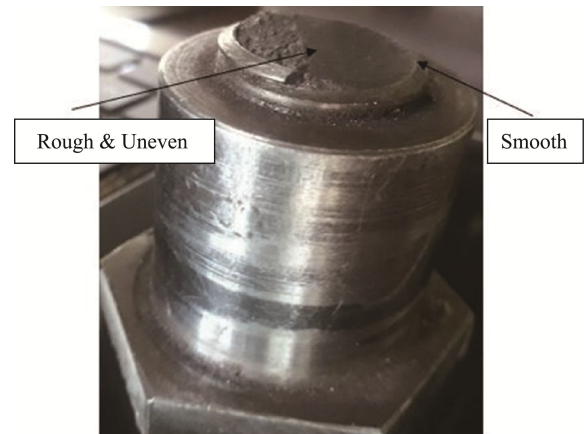
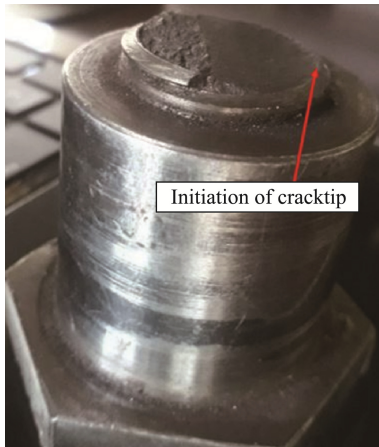


Fig.3 Two Different Cross Sections

It is observed from the Fig.3, that there was a time period during which this component had experienced fracture but due to cyclic loading, the surface has been ploughed due to the repeated contact between the two surfaces<sup>[21-22]</sup>. This causes polishing of the surface to take place. The crack tip initiates at the position as indicated in Fig.4, provided below and Process of Crack propagation on the fracture surface is shown in Fig.5.

Crack propagation occurs, across the surface in the direction of the red arrow as indicated in Fig.5, above.

Brittle Area of the fracture surface is shown in Fig.6



**Fig.4 Initiation of the Crack Tip on the Fracture Surface**



**Fig.5 Process of Crack Propagation on the Fracture Surface**



**Fig.6 Brittle Area of the Fracture Surface**

A relatively smooth surface was observed for approximately around 75% of the total fracture surface. This was associated with striations of a propagating ductile fatigue crack. A rough and uneven texture that was associated with the final brittle fracture, was observed on the remaining 25% of the total fracture surface. Noticeable deformation was observable in final failure. Presence of several possible crack initiation sites was visible on the fracture surface though they cannot be easily identified due to the shiny nature of the surface, but it was one main crack which lead to the failure. Presence of beach marks on the main crack were representations of it being a typical propagating fatigue crack. The cause of this propagating fatigue crack is most likely to be the mechanical damage incurred by the fracture surface due to the opening and closing of the fracture prior to final failure. The position of the initiation of the cracks was at a diameter transition in close proximity to the thread. The location of the area of the final failure is approximately at a 150 offset from that of the associated beach marks of the main crack.

In a fatigue failure, there are three steps. Initially it begins with a crack initiation. This can be due to surface defects and scratches on the surface. The initiated crack starts to propagate, causing beach marks relatively perpendicular to the direction of crack initiation. Finally, a combination of a reduction in area and a high stress concentration factor, leads to the occurrence of fracture which eventually causes the complete failure of the specimen. By observing the failed component, a rough area with less cross section was identified and a smooth area of more cross section since the specimen was under a cyclic torsion and a bending moment. It is assumed that the shined area was due to the relative motion of surfaces which was caused by torsion thereby while crack propagation was taking place, the beach marks were worn out and left with a shiny surface.

Since the specimen is hinged at the crank, in a slider crank mechanism, the total weight of the system is on that hinge, which acts as a bending moment. When it rotates, a torsion is induced by the friction of

the hinge. Cyclic loading failures are analyzed using several methods that include S-N curves for stress life approach,  $\epsilon$ -N curves for strain life approach and finally LEFM theories based on stress intensity factor. But with lack of resources, the approach is only based on stress life approach (S-N curves).

The S-N curves are based on general data and published data which makes it the easiest approach. The theory focuses on designing components for infinite life by preventing crack initiation with strength criteria, but this does not describe crack growth. Cyclic loads are classified into two types based on its mean value. For loads which the mean value is equal to zero, are analyzed using S-N curves and the loads which the mean value is not equal to zero are analyzed using Goodman diagrams. In this case, the specimen has experienced a constant load on the hinge which causes a bending moment, when the crank rotates the hinge experiences a sinusoidal change of bending moments acting on it. Therefore, our analysis neglected the Goodman diagram. Goodman diagrams originated from S-N curves. Those are, Gathering Data, Maximum yield strength, Maximum tensile strength, Surface finish factor, Reliability factor, Loading factor, Ideal endurance limit, Diameter of the crank, Length and weight of the rod, Weight of the blade, Simulations, Bending Stress, Pre-Calculations, Area, Mean Stress, Alternating stress, Corrected endurance limit, Drawing of S-N diagram, Drawing of Goodman diagram, Modified Goodman diagram, Determination of factor of safety and Determination of suitable diameter for a predefined safety factor.

For simplification of calculation purposes, the above two-dimensional arrangement was drawn using the actual data. The blade comes down at an angle of  $80^\circ$  with respect to the horizontal axis and the crank does all the work regarding its upwards and downwards, motion. While performing this work, the hinge takes part of the bending moment created by the force on it, with respect to the travelling direction of the blade. Using velocity and acceleration diagram, it was obtained, that the maximum velocity occurring at the crank angle is at  $10^\circ$  and  $190^\circ$ , to the horizontal axis.

Since the direction of the velocity of the crank (point B), is the same as that of the blade's velocity and the direction of its travel, the maximum speed occurs at those points. Dimensions & Arrangement of the system is shown in Fig.7.

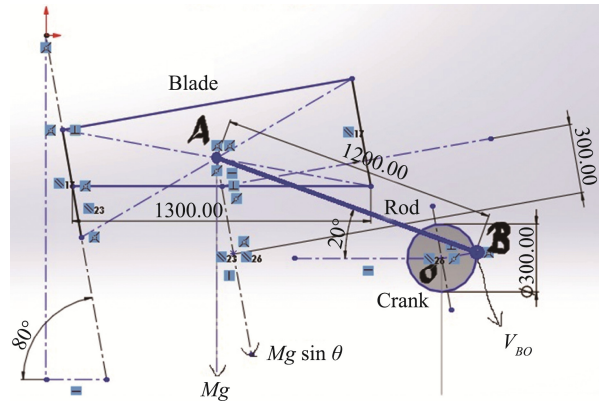


Fig.7 Dimensions & Arrangement of the System

Initially it was obtained that the crank takes 0.9 seconds to complete one complete cycle. In accordance to this obtained value, the speed of point B was calculated as  $7 \text{ rads}^{-1}$ . Finally, the force required to move the blade was calculated by using the law of conservation of momentum. Finalized Free Body Diagram is shown in Fig.8.

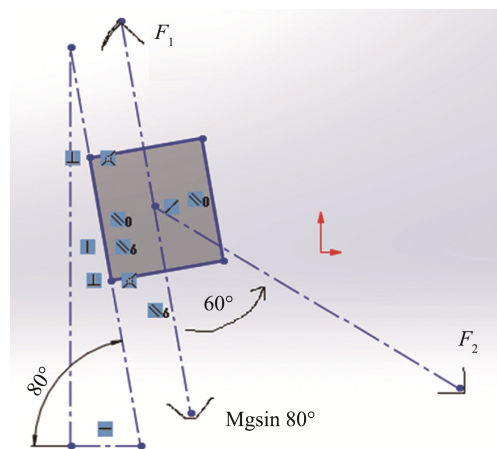


Fig.8 Finalized Free Body Diagram

$$F = \frac{mv - mu}{t} \tag{2}$$

along the line of  $80^\circ$

Downward to the horizontal axis

$$F_2 \cos 60^\circ = F_1 \quad (3)$$

Using equation (2), the required force on the blade, that is needed to change its direction, is calculated as 467 N. Considering the free body diagram using equation (3), the total force along the line of the

crank rod as 934 N was observed. The addition of the weight component along the line of the rod enables the total force to reach 1426 N. The effect of any frictional forces was neglected, during the calculations. The maximum force acting on the blade, is 1426 N. Cyclic Force on Hinge is shown in Fig.9 and Solidworks CAD Model is shown in Fig.10.

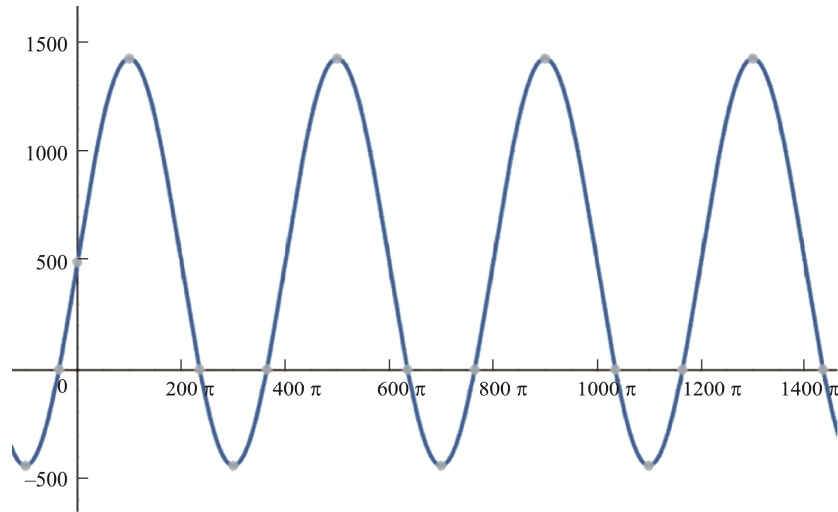


**Fig.9 Cyclic Force on Hinge**

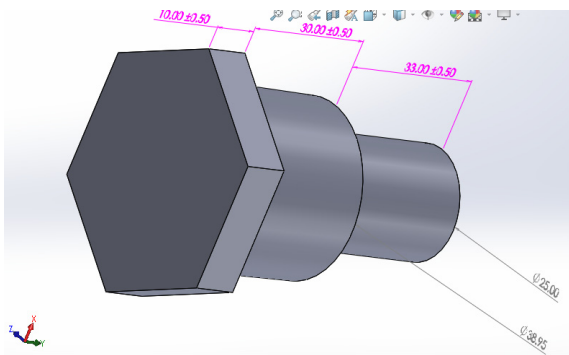


**Fig.10 Solidworks CAD Model**

## 4 Analysis

When considering Fig.8, it is very clear that the hinge is experiencing cyclic loading, which has a non-zero mean value. For further calculations, the maximum load on the hinge was needed in order to create the maximum principal stress on the hinge. Using a

static structural model created via ANSYS, it was able to obtain the maximum principal stress on the hinge, which is 9.49 MPa.

### Data

1. Structural Steel
  - a. Maximum Tensile Strength = 360 MPa
  - b. Maximum Yield Strength = 240 MPa
2. Factor of Safety = 3 (6 for static approximation)
3. Surface Finish = 63  $\mu$  inches (Critical lathe finish)
4. Loading Factor = 0.7
5. Size Factor = 1
6. Temperature Factor = 1
7. For 95% reliability; reliability factor = 0.868
8. Design for the room Temperature
9. Number of cycles for the design

Life cycle S-N Diagram is shown in Fig.11.

The ideal endurance limit of a material is determined by dividing the maximum strength into half. The corrected endurance limit is obtained using multiplying factors of loading, sizing, finishing, reliability, which are less than one, with the ideal endurance limit. Now the alternating stress component can be determined by according to the equation (4).

Data

1. Fatigue Strength Coefficient = 564.4 MPa<sup>[4]</sup>

2. Fatigue Strength Component (b) = - 0.0576<sup>[4]</sup>

$$\sigma_A = \sigma'_F \cdot (2 \times N)^{-b} \quad (4)$$

Hence, the Goodman diagram can be drawn using

above data. Goodman Diagram is shown in Fig.12.

According to the simulation results of the specimen, using ANSYS, the maximum principal stress as, 3.6 MPa and the minimum principal stress as, 1.2MPa were obtained. Using the minimum and maximum forces as, 467N and 1476N.

Goodman Diagram describes the interplay of mean stress with alternating stress at failure, on a given number of cycles.

$$\sigma_{mean} = \frac{\sigma_{MinMax}}{2} \quad (5)$$

$$\sigma_A = \sigma_{Max} - \sigma_{mean} \quad (6)$$

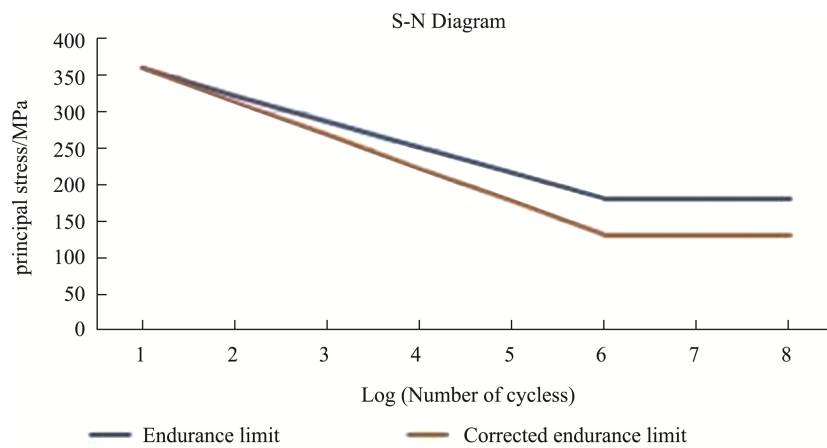


Fig.11 S-N Diagram

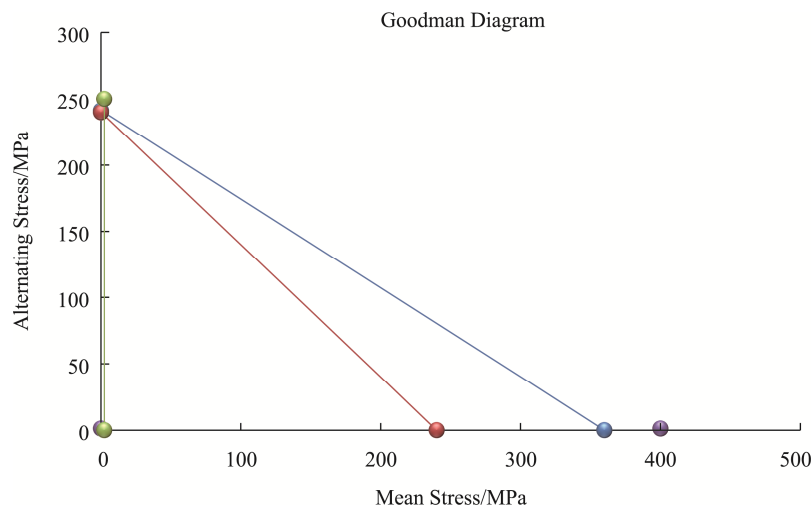


Fig.12 Goodman Diagram

According to the equation (5) and (6), Mean Stress was 2.4 MPa and Alternating Stress was 1.2 MPa. Using the ANSYS engineering data of structural steel, the following S-N curve was obtained which is almost similar to our theoretically obtained S-N curve. Similarly, the curve knees on  $10^6$  cycles. ANSYS derived S-N Diagram is shown in Fig.13.

In the finite element model, the patch confirming method was used to create the mesh with tetrahedral elements due to the uneven shape of the specimen and the mesh size being set to default. After the introduction of a minimized sizing method, the results did not show any deviation, therefore the results shown in this section are based on the patch confirming method.

The boundary condition was set to fixed support for the curved area of the smaller diameter belonging to the specimen and a vector component is defined along

the Y-axis, as the acting force, to cause the bending moment. Using the fatigue tool of ANSYS, a cyclic load was developed with the loading type chosen as the ratio and substituting values for the loading ratio and scale factor as 0.316 and 1, respectively.

The solution was developed using fatigue analysis life set to stress life as well as the mean stress theory set to Goodman, fatigue strength factor set to 1. The results of the solution were taken as life, safety factor and fatigue sensitivity using fatigue tools and after equivalent stress, total deformation and maximum principal stress. Stress Life approach using Goodman Diagram is shown in Fig.14.

Ratio and the Scale Factor Data Entered is shown in Fig.15, Applied Force and its direction is shown in Fig.16 and Fixed Support for the Minor Diameter Surface is shown in Fig.17.

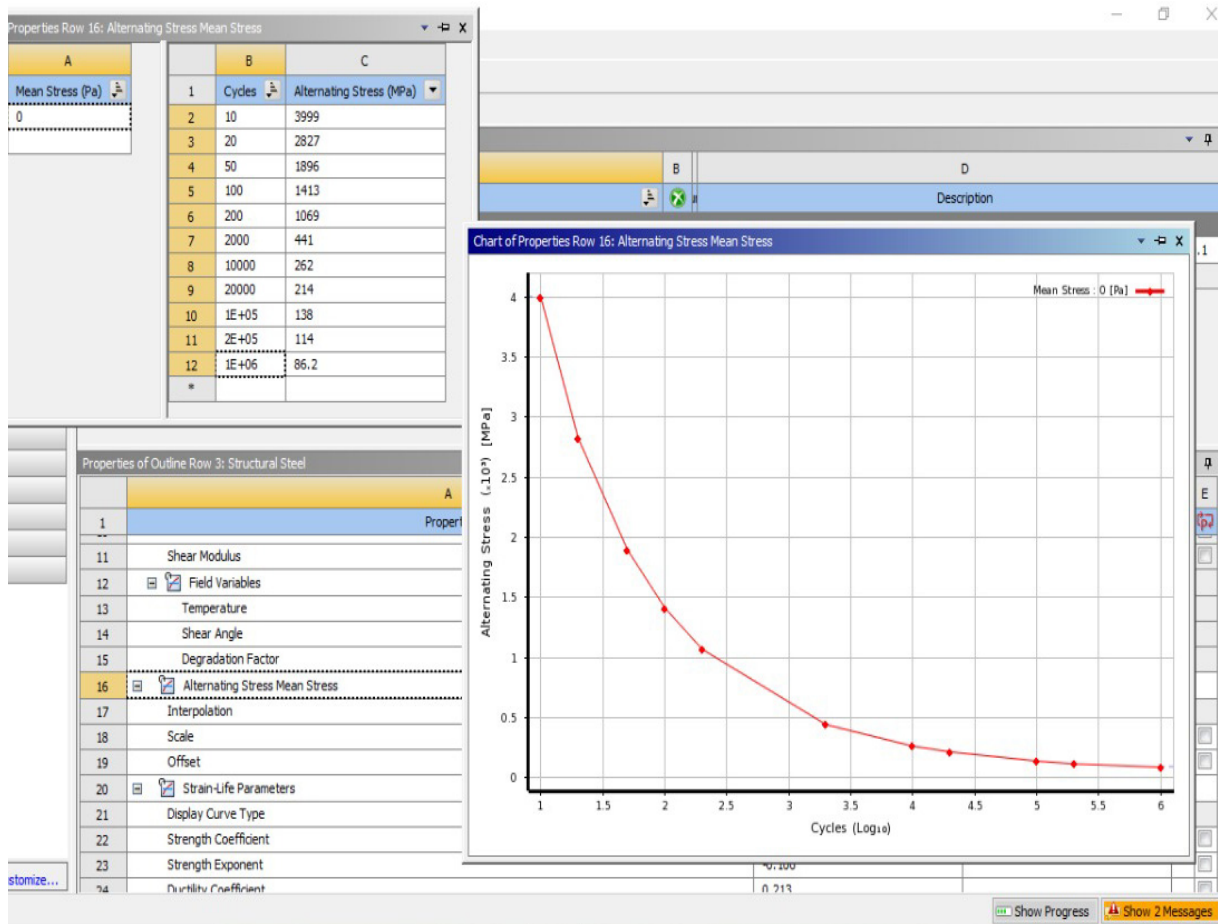
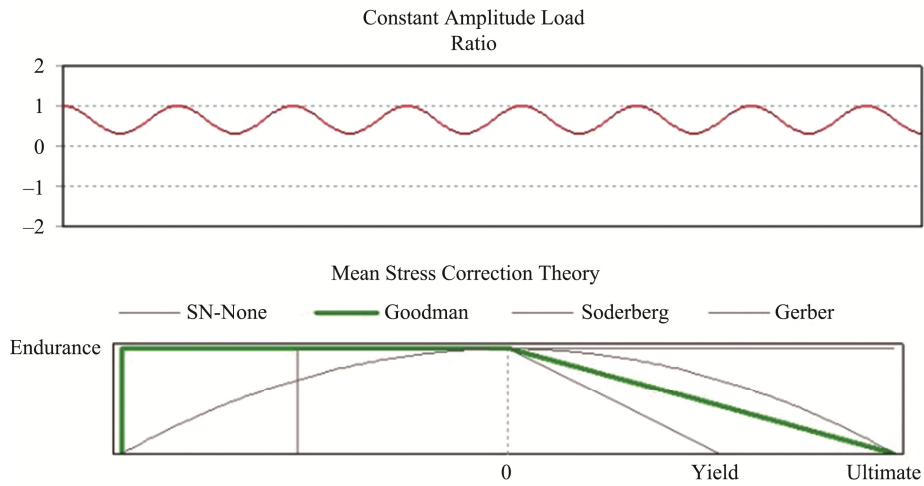
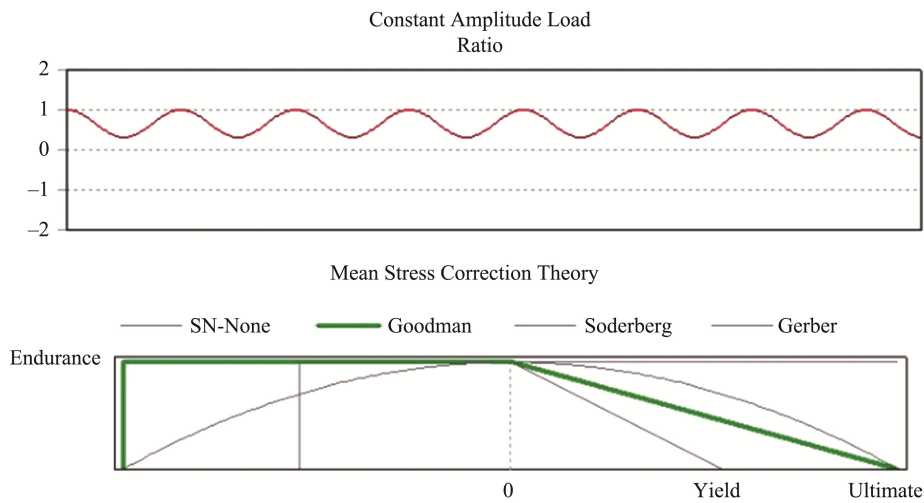


Fig.13 ANSYS Derived S-N Diagram



**Fig.14 Stress Life Approach Using Goodman Diagram**



**Fig.15 Ratio and the Scale Factor Data Entered**

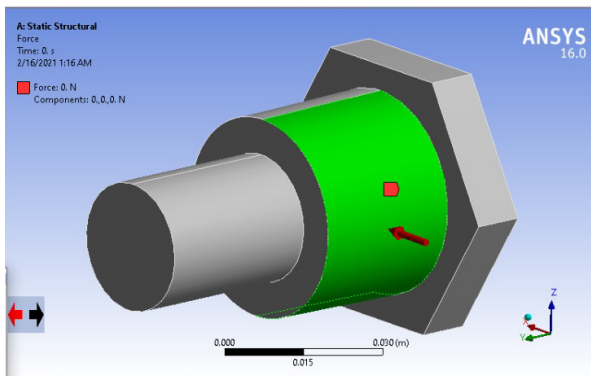


**Fig.16 Applied Force and Its Direction**

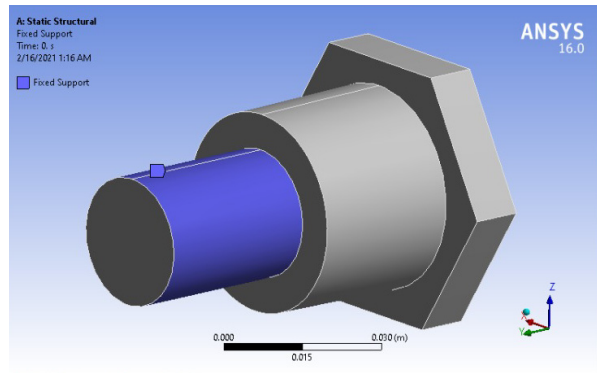


**Fig.17 Fixed Support for the Minor Diameter Surface**

### 5 Results & Discussion

As per the Goodman diagram, by plotting a vertical line along the point of 1.2, of the mean stress axis, a factor of safety for tensile stress of approximately 200, was obtained. Similarly, a factor of safety of approximately 200, was obtained, considering the tensile strength. At the beginning of this research, the force calculations were highly dependent on the force diagrams data and the weight of the blade and the friction of the surfaces and negligence of torsional forces on the hinge. Therefore, the resultant data, did not denote any clue of failure.

The cause of failure might be due to the occurrence of a combination of bending moments and torsional stresses but due to lack of data on the torsional stress, the research’s focus was narrowed down to effects and analysis of the bending moments. Another consideration is the force it requires to make the cut of thousand or two thousand paper sheets were also not included. Sensing or detecting the torsional stresses, friction force, installation errors, & Cutting Jerk requires more expensive investigation and instrumentation. Also, there can be an integrated offset force due to wear and tear of old machine parts. Reasons behind these obtained highly unusual large values of safety factor can be due to above mentioned scenarios. Even with the increase of loading by 1500% in the fatigue sensitivity graph, a reduction in the number of cycles to the failure, was barely observed. Fatigue Sensitivity Curve is shown in Fig.18.

This indicates that the reason behind the frequent failure of the hinge was not caused by the bending moments. As recommendations for a higher fatigue life of the hinge are constant lubing of machine parts, take great care while installing them, and execute preventive maintenance for greater machine part life, so the wearing are issues crated by them wont effect to the fatigue life of the hinge. Fatigue Life is shown in Fig.19, Fatigue Safety Factor is shown in Fig.20, Maximum Principal Stress is shown in Fig.21 and Total Deformation is shown in Fig.21.

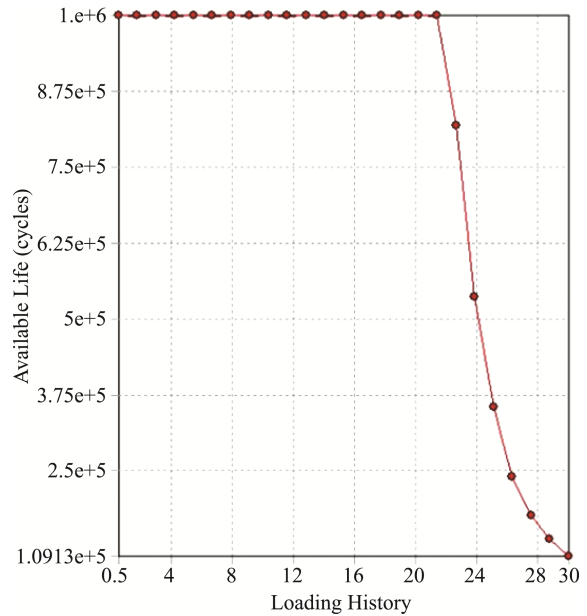


Fig.18 Fatigue Sensitivity Curve

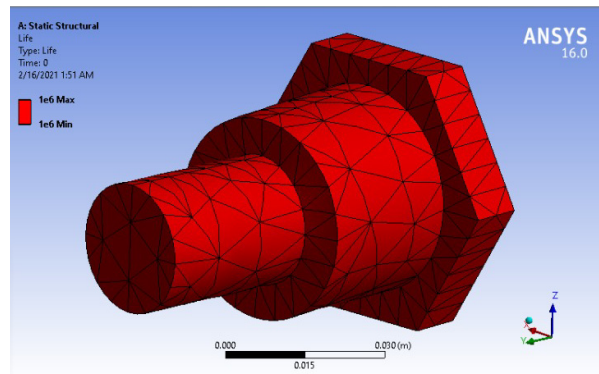


Fig.19 Fatigue Life

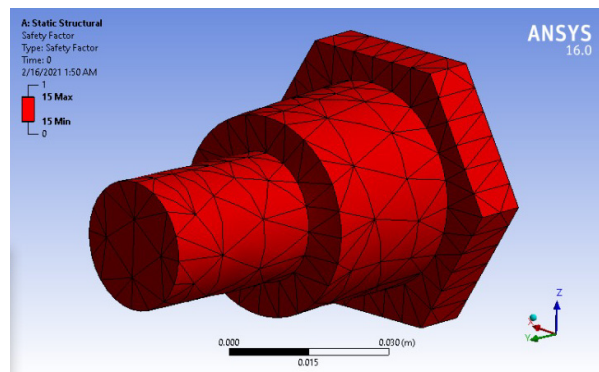


Fig.20 Fatigue Safety Factor

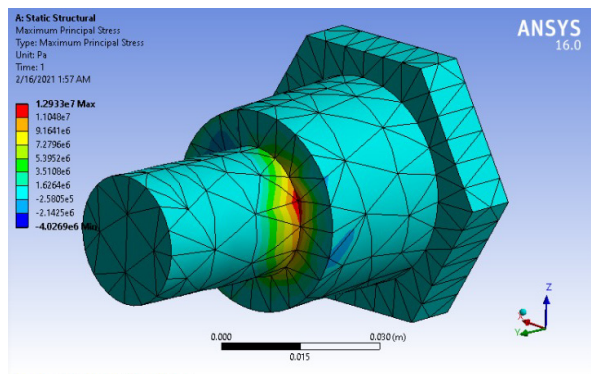


Fig.21 Maximum Principal Stress

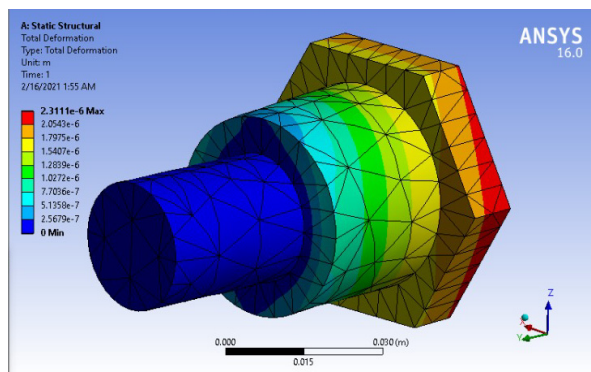


Fig.22 Total Deformation

## 6 Conclusion

The mode of failure of the hinge is fatigue which caused under cyclic loading conditions. Clear evidences are shown in the fracture surface to prove the fatigue failure. But the stress analysis shows the maximum stress induced on the hinge at working conditions are well below the fatigue endurance limit. Further investigations are needed to conclude the course of failure. It could be due to material imperfection or failure could be initiated from an embedded foreign particle at the surface of the hinge which needs SEM investigation to prove. Also, it could be any form of surface defect which could be occurred at the time of assembling the hinge. There is a possibility of having an impact load or sudden jerk on the hinge due to some operational malfunction.

Failure analysis is always giving unexpected re-

sults which needs further investigations. But the important aspect of it is that these investigations indicate at least minor scientific evidences which lead to prevent such failures.

## References

- [1] Society of Automotive Engineers, S., 1986. SAE Fatigue Design Handbook. 3rd ed. Illinois: Society of Automotive Engineers.
- [2] Tawancy, H., Hamid, A. and Abbas, N., 2004. Practical Engineering Failure Analysis. 1st ed. New York: Marcel Dekker Inc.'
- [3] Cui, W., 2001. A state-of-the-art review on fatigue life prediction methods for metal structures. Journal of Marine Science and Technology, [Online]. DOI: 10.1007/s007730200012,2,3. Available at: [https://www.researchgate.net/publication/225664300\\_A\\_state\\_of\\_the\\_art\\_review\\_on\\_fatigue\\_life\\_prediction\\_methods\\_for\\_metal\\_structures](https://www.researchgate.net/publication/225664300_A_state_of_the_art_review_on_fatigue_life_prediction_methods_for_metal_structures) [Accessed 14 February 2021].
- [4] Pan WF, Hung CY, Chen LL (1999) Fatigue life estimation under multiaxial loadings. Int J Fatigue 21:3–10.
- [5] Foreman RG, Kearney VE, Engle RM (1967) Numerical analysis of crack propagation in cyclic-loaded structures. J Basic Eng 89:459–464.
- [6] Cruces, A., Crespo, P., Moreno, B. and Antunes, F., 2018. Multiaxial Fatigue Life Prediction on S355 Structural and Offshore Steel Using the SKS Critical Plane Model. MDPI, [Online]. Metals 2018, 8, 1060, 2 & 3. Available at: <https://www.mdpi.com/2075-4701/8/12/1060> [Accessed 14 February 2021].
- [7] Wang, E., Nelson, T. and Rauch, R., 2004. Back to Elements - Tetrahedra vs. Hexahedra. CAD-FEM GmbH, [Online]. CAD-FEM, 2-14. Available at: <https://docplayer.net/21829223-Back-to-elements-tetrahedra-vs-hexahedra.html> [Accessed 14 February 2021].
- [8] V.J. Colangelo and F.A. Heiser, Analysis of Metallurgical Failures (2nd ed.), p. 66 John Wiley and Sons, Inc., 1987.
- [9] Julie A. Bannatine, Jess J. Comer, James L. Handrock, Fundamentals of Metal Fatigue Analysis, Prentice Hall, Englewood Cliffs, New Jersey 07632, ISBN 0-13-340191-X.
- [10] Suresh S. Fatigue of Materials, 2nd Edition, University of Cambridge, Cambridge, 1998; ISBN 0-521-57847-7.
- [11] Mughrabi H, Microscopic Mechanisms of Metal Fatigue,

- Strength of metals and alloys (Edited by P. Haasen, V. Gerold, and G. Kostorz), 1980; vol. III (Pergamon, Oxford) p. 1615-38.
- [12] David Taylor, Modelling of Fatigue Crack Growth at the Microstructural Level, Computational Materials Science, 25 (2002) 228-236.
- [13] Ong JH (1993) An improved technique for the prediction of axial fatigue life from tensile data, Int J Fatigue 15:213-219.
- [14] Miller KJ. O'Donnell WJ., The fatigue limit and its elimination, Fatigue Frac Engng Mater Struct, 22, 545-57, 1999.
- [15] Bathias C., There is no infinite fatigue life in metallic materials, Fatigue Frac Engng Mater Struct, 22, 559-65, 1999.
- [16] Fatigue and Fracture, ASM handbook, Volume 19, ASM International, 1996; ISBN 0-87170-385-8.
- [17] Fatigue Design Handbook, Second Edition, Society of Automotive Engineers, Inc., 1988; ISBN 0-89883-011-7.
- [18] Fujimoto Y, Hamada K (2000) Propagation and non-propagation of small fatigue cracks. Proceedings of the 10th International Offshore and Polar Engineering Conference, Seattle, USA, May 28–June 2, pp 180–187.
- [19] Brown LM, Ogin SL, Role of internal stress in the nucleation of fatigue cracks, Theory of Materials Group, University of Sheffield.
- [20] Mughrabi H, Microscopic Mechanisms of Metal Fatigue, Strength of metals and alloys (Edited by P. Haasen, V. Gerold, and G. Kostorz), 1980; vol. III (Pergamon, Oxford) p. 1615-38.
- [21] Kocanda S (1978) Fatigue failures of metals. Sijthoff and Noordhoff, International Publishers, Netherlands
- [22] Forsyth PJE (1969) The physical basis of metal fatigue. American Elsevier, New York.

### Author Biographies



**A. R. LOKUGE** received his BEng (Hons) degree in Mechanical Engineering from Kingston University, London and B. Tech. Eng. (Hons) degree in Mechatronics Engineering from the Open University of Sri Lanka.

E-mail: randimaaruna@gmail.com



**R. J. WIMALASIRI** received his B. Tech. Eng. (Hons) degree from the OUSL and Ph.D. degree from Sheffield Hallam University, United Kingdom. He is currently a Senior Lecturer in Mechanical Engineering at OUSL. His main research

interest includes structural integrity of machine elements.

E-mail: rjwim@ou.ac.lk



**Copyright:** © 2021 by the authors. This article is licensed under a Creative Commons Attribution 4.0 International License (CC BY) license (<https://creativecommons.org/licenses/by/4.0/>).